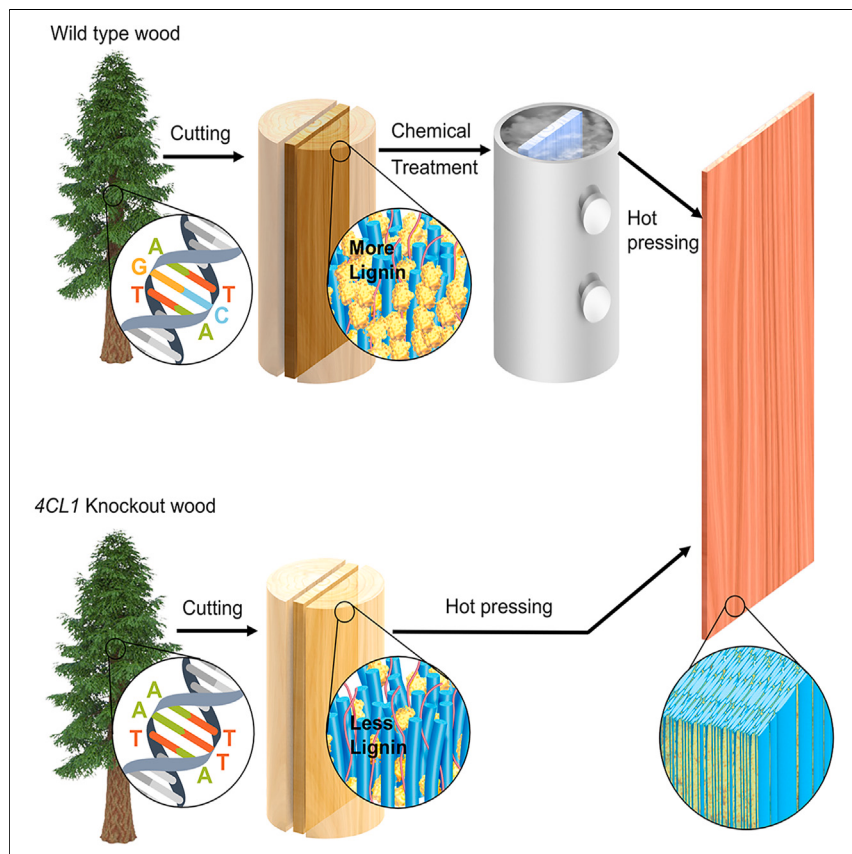


Article

Genome-edited trees for high-performance engineered wood



Conventional delignification uses chemicals that consume a lot of energy and create significant waste, posing sustainability issues. By using genome-edited poplar trees with lower lignin content, we can skip the chemical delignification process. This innovative approach reduces environmental impact and offers a more sustainable solution for processing engineered wood.

Yu Liu, Gen Li, Yimin Mao, ...,
Xuejun Pan, Yiping Qi,
Liangbing Hu

yiping@umd.edu (Y.Q.)
binghu@umd.edu (L.H.)

Highlights

Reducing the lignin in polar wood by knocking out the *4CL1* gene

Demonstrating a chemical-free method for processing advanced engineered wood

Densified *4CL1* knockout wood is as strong as densified wood from chemical treatment



Development

Practical, real world, technological considerations and constraints

Liu et al., Matter 7, 1–14

October 2, 2024 © 2024 Elsevier Inc. All rights reserved, including those for text and data mining, AI training, and similar technologies.
<https://doi.org/10.1016/j.matt.2024.07.003>

Article

Genome-edited trees for high-performance engineered wood

Yu Liu,^{1,7} Gen Li,^{2,7} Yimin Mao,^{1,3} Yue Gao,^{1,7} Minhua Zhao,¹ Alexandra Brozena,¹ Derrick Wang,¹ Samuel von Keitz,¹ Taotao Meng,¹ Hoon Kim,⁴ Xuejun Pan,⁵ Yiping Qi,^{2,6,*} and Liangbing Hu^{1,8,*}

SUMMARY

Replacing conventional structural materials with high-performance engineered wood can reduce CO₂ emissions and enhance carbon sequestration. Traditional methods involve energy-intensive chemical treatments to reduce lignin content, resulting in denser, mechanically superior wood but raising sustainability concerns. This work introduces a genome-editing approach to reduce lignin in trees, enabling chemical-free processing of advanced engineered wood. Using the cytosine base editor nCas9-A3A/Y130F, the 4CL1 gene in poplar wood was targeted, achieving a 12.8% lignin reduction. This facilitated waste-free densified wood production through water immersion and hot pressing, yielding a tensile strength of 313.6 ± 6.4 MPa, comparable to aluminum alloy 6061. The strength of densified 4CL1 knockout wood closely matched that of traditionally treated wood (320.2 ± 3.5 MPa), demonstrating the effectiveness of genetic modification in creating sustainable, high-performance engineered wood and contributing to reduced CO₂ emissions and environmental conservation.

INTRODUCTION

Engineered wood is increasingly being explored as a sustainable alternative to conventional structural materials, such as steel, cement, glass, and plastic.^{1,2} Such advanced wood materials offer unique properties, such as high mechanical strength,^{3,4} passive radiative cooling,⁵ and light management,^{6–8} which is achieved by controlling wood's naturally anisotropic structure through various methods. Wood is made up of several components, including the polymer lignin that binds the cellulose fibers of the wood cell walls to impart structural strength as well as defense against pathogens.⁹ Successfully fabricating high-performance engineered wood materials typically requires the partial or complete removal of lignin from the wood feedstock in order to enable subsequent treatments that modify the natural wood structure, such as densification for enhanced mechanical properties^{3,4} or tuning of the optical absorption.^{5,10} However, the delignification process is generally achieved using a variety of chemical approaches (e.g., NaOH, NaOH/Na₂SO₃, NaOH/Na₂S, NaClO₂, etc.) that are energy intensive and generate significant waste, posing sustainability challenges.^{4,7,8,10–12} Therefore, a more sustainable yet still cost-effective method of reducing the lignin content in natural wood is needed for the manufacturing of engineered wood.

Several alternative chemistries and approaches have been explored for more sustainable methods of lignin removal in the production of advanced wood materials,

PROGRESS AND POTENTIAL

We demonstrated a waste-free process for processing engineered wood by reducing the lignin content of poplar wood through 4CL1 knockout technology. The 4CL1 knockout wood shows a 12.8% reduction in lignin content without significant growth changes. By soaking this wood in water and hot pressing, we achieved a tensile strength of 313.6 ± 6.4 MPa, 5.6 times higher than that of natural 4CL1 knockout wood and 1.6 times higher than that of densified wild-type wood. This strength is comparable to chemically treated densified wood (320.2 ± 3.5 MPa). Our method eliminates chemical delignification, offering a cost-effective, eco-friendly alternative for producing densified wood. This success highlights genome editing's potential to create other engineered wood materials with enhanced properties, contributing to a CO₂-negative bioeconomy by providing renewable alternatives to traditional materials.

including organosolv pulping,^{13,14} the use of ionic liquids,¹⁵ microwave-assisted methods,¹⁶ and enzymatic delignification.¹⁷ However, challenges still persist in terms of efficiency, energy use, and waste products.¹⁸ In addition to alternative chemistries, genetic engineering techniques have been applied in the paper and pulp industry to modify the lignin content and composition in trees used for pulp production. For example, knocking out genes involved in lignin synthesis, such as 4CL1 (e.g., 4CL1-1 and 4CL1-2),^{19–21} C3H3, CAD1, and AldOMT2,²² can be an efficient way of reducing the lignin content in wild-type wood for enhanced mechanical properties of the pulp fibers.²³ However, further research and development are needed to explore the applicability, sustainability, and performance of 4CL1 knockout trees for engineered wood production.

In this study, we demonstrate the waste-free synthesis of high-strength engineered wood using 4CL1 knockout poplar that features a lower lignin content, thus avoiding the need for chemical delignification (Figure 1A). Our previous study has demonstrated the CRISPR-based cytosine base editor nCas9-A3A/Y130F system as a robust genome engineering tool in poplar wood, which allows up to 95.5% editing efficiency.^{24,25} With this technique, we reduced the lignin content by knocking out a key gene (4CL1) of lignin biosynthesis, specifically using two guide RNAs (gRNAs) to target the first exon of the 4CL1 gene to introduce pre-mature stop codons (Figures S1A and S1B). With this approach, the resulting 4CL1 knockout wood featured a 12.8% lower lignin content compared to the wild-type feedstock, which is comparable to chemical-based methods of delignification for fabricating engineered wood products.³ As a proof of concept, we used the 4CL1 knockout wood to fabricate high-strength densified wood by soaking the material in water under vacuum, followed by hot pressing (Figure 1B). Due to the lower lignin content, the cell walls are able to collapse and form a denser structure, with greater hydrogen bonding between the cellulose chains. As a result, the densified 4CL1 knockout wood exhibits a remarkable tensile strength of 313.6 ± 6.4 MPa, which is 5.6 times higher than that of the 4CL1 knockout wood prior to densification (56.1 ± 12.0 MPa) (Figure 1C). Moreover, the densified wood's tensile strength is on par with that of aluminum alloy 6061.²⁶ In addition, a densified wood was prepared from wild-type wood using the traditional process involving chemical treatment to eliminate 12.4% of lignin,³ akin to the genome-editing process, followed by hot pressing. The resulting densified wood exhibits a tensile strength of 320.2 ± 3.5 MPa, comparable to the tensile strength of densified 4CL1 knockout wood (Figure 1C). These findings demonstrate that reducing the lignin content in wood via genetic engineering is a viable strategy for densified wood manufacturing, with the potential for tailoring the lignin content and composition to meet the specific requirements of different engineered wood materials. This genetic engineering approach avoids the need for chemical delignification treatments and thus prevents the generation of waste, offering a cost-efficient and eco-conscious approach to manufacturing engineered wood.

RESULTS AND DISCUSSION

Lignin is a polymer composed of three monomers, *p*-hydroxyphenyl (H), guaiacyl (G), and syringyl (S),²⁷ which are synthesized from phenylalanine through multiple metabolic steps and enzymes.²⁸ 4CL1 is one of the critical enzymes of the lignin biosynthesis pathway, and knocking down or knocking out 4CL1 has been shown to reduce the lignin content of stem wood in poplar.^{24,29,30} Our previous study demonstrated that the nCas9-A3A/Y130F-based C-to-T base editing system allows for up to 95.5% editing efficiency.^{24,25} To achieve homozygous 4CL1 knockout

¹Department of Materials Science and Engineering, University of Maryland, College Park, MD 20742, USA

²Department of Plant Science and Landscape Architecture, University of Maryland, College Park, MD 20742, USA

³NIST Center for Neutron Research, National Institute of Standards and Technology, Gaithersburg, MD 20899, USA

⁴US Department of Agriculture, Forest Service, Forest Products Laboratory, One Gifford Pinchot Drive, Madison, WI 53726, USA

⁵Department of Biological Systems Engineering, University of Wisconsin-Madison, 460 Henry Mall, Madison, WI 53706, USA

⁶Institute for Bioscience and Biotechnology Research, University of Maryland, Rockville, MD, USA

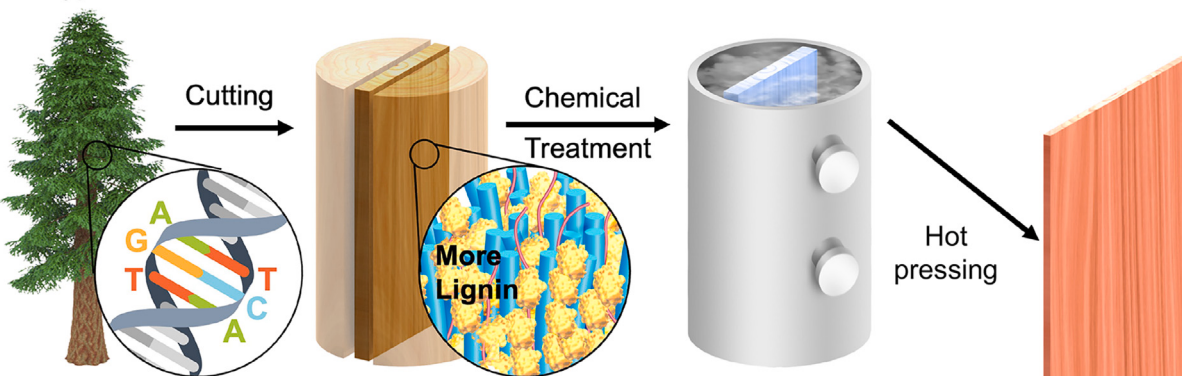
⁷These authors contributed equally

⁸Lead contact

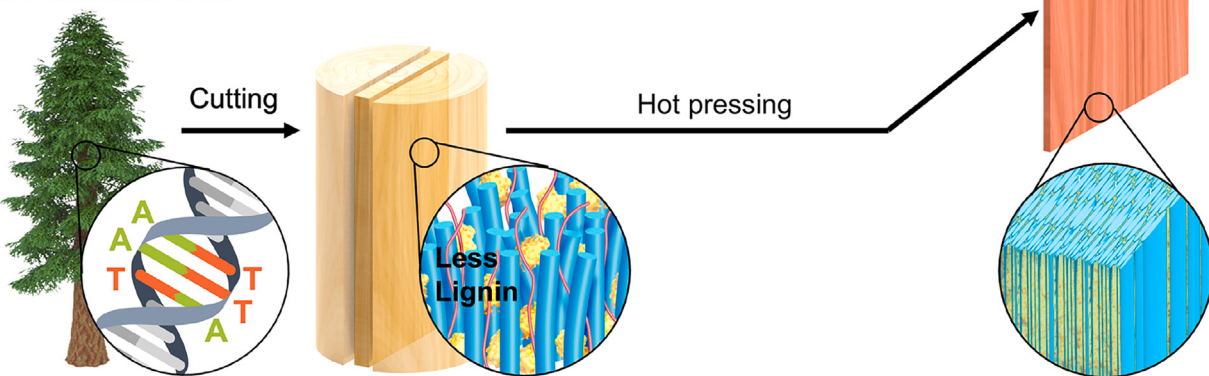
*Correspondence: yiping@umd.edu (Y.Q.), binghu@umd.edu (L.H.)

<https://doi.org/10.1016/j.matt.2024.07.003>

A Wild type wood



4CL1 Knockout wood



B

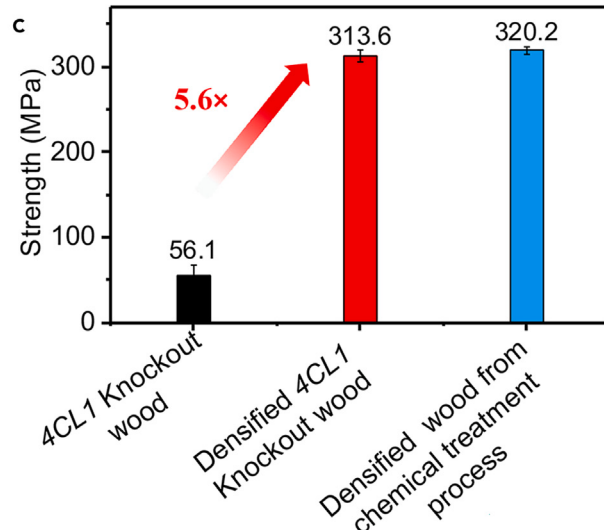
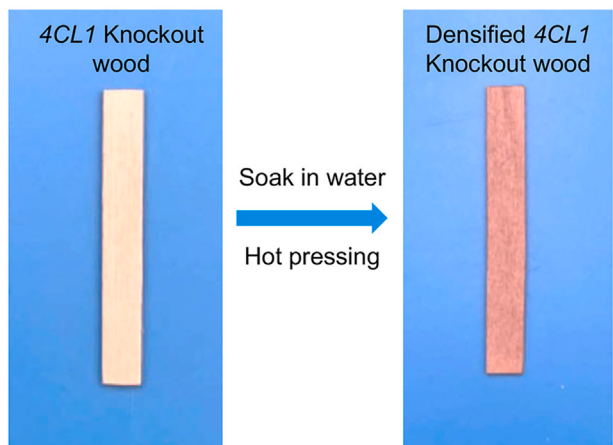


Figure 1. A genome-editing approach for fabricating high-strength densified wood

(A) The schematic depicts the contrast between conventional densified wood fabrication, which requires chemical treatment to partially remove lignin before densification, and the innovative waste-free process achieved through genetic engineering of the wood starting material to reduce the lignin content.

(B) The photos showcase the waste-free manufacturing process of densified 4CL1 knockout wood. The process involves soaking the wood in water, followed by densification.

(C) Comparison of the tensile strength of the 4CL1 knockout wood, the densified 4CL1 knockout wood, and the densified wood from chemical treatment process.

Data are represented as mean \pm SEM.

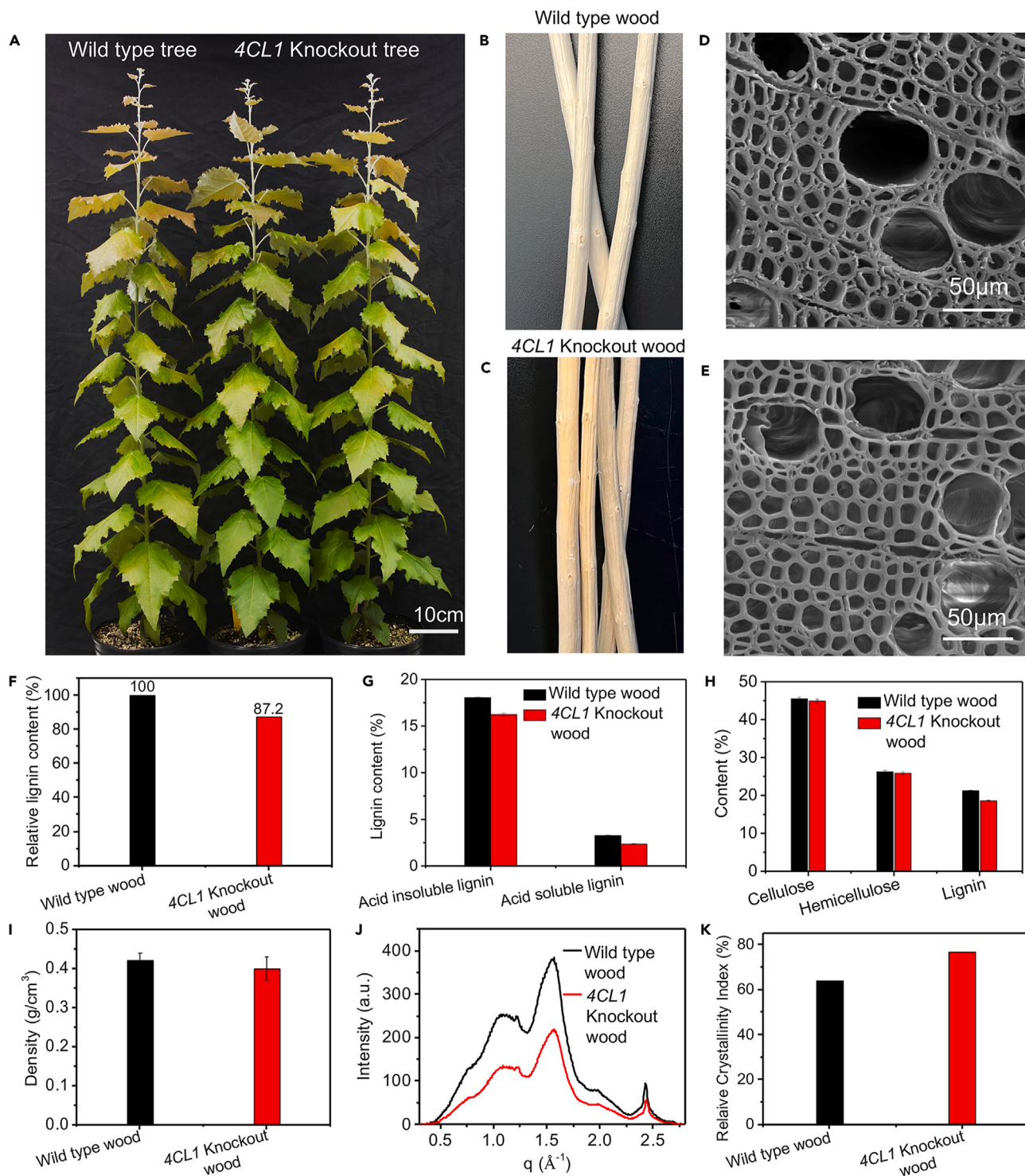


Figure 2. Physiological and physical characterization of the 4CL1 knockout trees for wood engineering

(A) Photo of the wild-type poplar and 4CL1 knockout tree after growing in a greenhouse for 6 months.

(B and C) Photographs of the dry (B) wild-type wood and (C) 4CL1 knockout wood.

(D and E) SEM images of the (D) wild-type wood and (E) 4CL1 knockout wood in cross-section show little change in fiber cell lumen, vessel diameter, or cell wall thickness.

(F) Comparison of the relative lignin content of the wild-type wood and 4CL1 knockout wood.

(G) Comparison of the acid-insoluble and acid-soluble lignin content of the wild-type wood and 4CL1 knockout wood.

Figure 2. Continued

(H) Comparison of the cellulose, hemicellulose, and lignin content of the wild-type wood and 4CL1 knockout wood.

(I) Comparison of the wild-type wood and 4CL1 knockout wood density.

(J) WAXD traces of the wild-type wood and 4CL1 knockout wood.

(K) Comparison of the crystallinity of the cellulose of the wild-type wood and 4CL1 knockout wood.

Data are represented as mean \pm SEM.

mutants, more transgenic plants were generated using this base editing system. Briefly, in the C-to-T base editing system, two gRNAs were used for targeting the first exon of the 4CL1 gene to introduce pre-mature stop codons (Figures S1A and S1B). The transfer DNA (T-DNA) vector was transformed into poplar explants using an *Agrobacterium*-mediated method. Regenerated T₀ plants were analyzed using Sanger sequencing to identify the genotype. Two homozygous mutants (4CL1-1 and 4CL1-2) were identified, and both were introduced with a pre-mature stop codon (Q213X) by biallelic C-to-T base editing (Figure S2). We did not observe any difference in the plant growth of the 4CL1 mutants compared to the unmodified poplar tree. After 6 months of growing in the same greenhouse environment, the 4CL1 knockout tree had grown almost the same amount as the wild-type tree (Figures 2A and S4). Mutating 4CL1 affects the change of lignin monomer combination, resulting in a darker wood color.²⁴ Therefore, while the fresh wild-type wood appeared light green, the fresh wood of the 4CL1 mutants featured a reddish color (Figure S3), similar to previous studies.^{24,29} In its dry state, wild-type wood maintains a white color (Figure 2B), whereas the wood from the 4CL1 mutants adopts a light yellow hue (Figure 2C).

Furthermore, scanning electron microscopy (SEM) images of the cross-sections of both the wild-type wood (Figure 2D) and 4CL1 knockout wood (Figure 2E) samples reveal nearly identical sizes of the fiber cell lumen, vessel diameter, and cell wall thickness. In addition, the alignment of the cellulose fibers does not change after genome editing (Figure S5). This indicates that the genetic engineering process does not significantly alter the wood's microstructure. Figure 2F shows that the 4CL1 knockout wood exhibits a 12.8% decrease in lignin content compared with wild-type wood after mutating 4CL1. Specifically, the acid-insoluble lignin contents of the natural and 4CL1 knockout wood are 18.05% and 16.24%, respectively, which are approximately 10% decreases. Meanwhile, the acid-soluble lignin content of the 4CL1 knockout wood is 2.35%, which is a 28% decrease compared with the wild-type wood (3.27%), as shown in Figure 2G. Meanwhile, the natural and 4CL1 knockout wood samples feature similar cellulose and hemicellulose contents (Figure 2H). The wild-type wood and 4CL1 knockout wood also feature a similar density (0.42 and 0.40 g/cm³, respectively; Figure 2I). Fourier transform infrared spectroscopy (FTIR) shows that both samples feature essentially the same main characteristic peaks, indicating that the main chemical compositions of the two types of wood are identical (Figure S6). We also used the relative crystallinity index obtained from wide-angle X-ray diffraction (WAXD) traces (Figures 2J and S7–S9) as a measure to evaluate the cellulose content of the wild-type and 4CL1 knockout wood. The WAXD traces can be decomposed into two portions, contributed by the crystalline (mainly cellulose) and amorphous (mainly lignin and hemicellulose) phases, which are represented by a group of sharp Bragg peaks and a broad scattering halo, respectively.³¹ The relative crystallinity index is measured as a fraction of the crystalline phase scattered intensity over the total scattered intensity. The 4CL1 knockout wood shows a higher relative crystallinity index of 76.8% compared with that of wild type, 64.1% (Figure 2K). We attribute the increase of the relative crystallinity index by 12.8% to the decrease of the lignin content. One of the concerns associated with the decrease of lignin content is that it might cause a decrease of the degree of cellulose

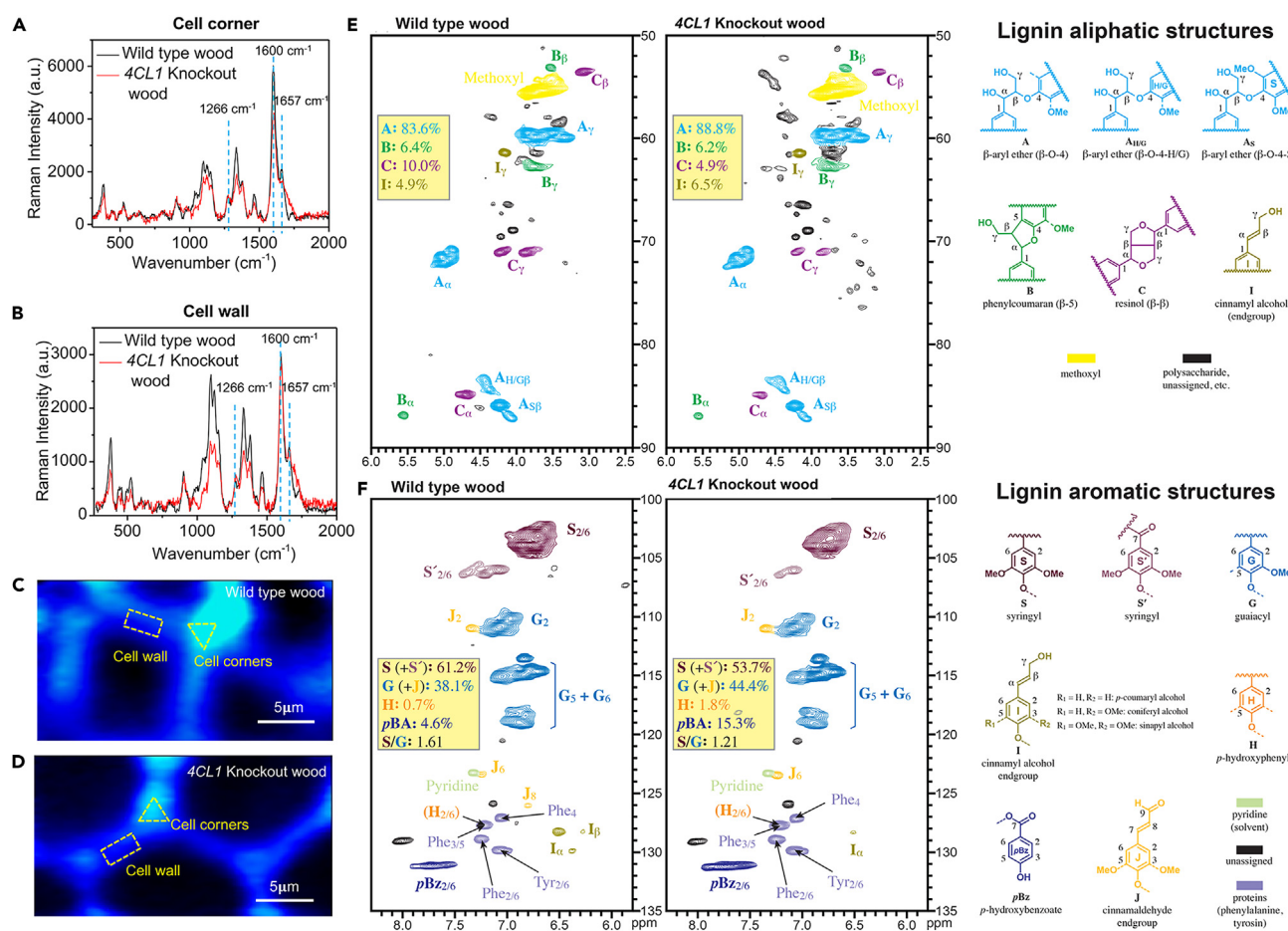


Figure 3. Distribution and structure of lignin characterization by Raman spectra and 2D HSQC.

(A and B) The Raman spectra of (A) cell corners and (B) cell walls to compare characteristic bands of lignin at 1,266, 1,600, and 1,657 cm⁻¹ between wild-type wood and 4CL1 knockout wood.

(C and D) Raman mapping of (C) wild-type wood and (D) 4CL1 knockout wood to compare the lignin distribution in these two types of wood.

(E and F) 2D HSQC NMR spectra were employed to compare the structural changes in lignin between (E) wild-type wood and (F) 4CL1 knockout wood. The spectra were analyzed for both aliphatic regions (δC/δH 50–90/2.5–6.0) and aromatic regions (δC/δH 100–135/5.9–8.2) to gain insights into the modifications in lignin composition resulting from the genome-editing process.

fiber alignment, consequently yielding a decreased mechanical performance. We calculated the degree of cellulose fiber orientation in natural and 4CL1 knockout wood using Hermans orientation factor P_2 , determined from the polar angle distribution of the scattered intensity of the 2D WAXD pattern (see Figure S10A for wild-type wood and Figure S10B for 4CL1 knockout wood). The P_2 values of the wild type and 4CL1 knockout wood were 0.95 and 0.91, respectively (Figure S10C), suggesting that the cellulose microfibrils are slightly less aligned in the 4CL1 knockout wood than in the wild type,³² but they are generally on the same level, and the slight difference should not cause a significant variation in mechanical performance. All these results demonstrate that genome editing has little influence on the physical properties and behavior of the wood (e.g., tree growth) except for an observed decrease in the lignin content.

We used Raman spectroscopy to investigate how the lignin distribution changes after genome editing. The characteristic bands of lignin appear at 1,266, 1,600, and 1,657 cm⁻¹ for both the wild-type and 4CL1 knockout wood samples (Figures 3A

and 3B).^{33–35} Notably, the lignin characteristic peaks (1,600 and 1,657 cm⁻¹) in the Raman spectra of the cell corners for 4CL1 knockout wood (Figure 3A) are lower compared to those of wild-type wood, indicating a reduction in lignin content in the cell corners after the genome-editing process. Conversely, the lignin characteristic peaks in the Raman spectra of the cell walls show no significant changes for either wild-type or 4CL1 knockout wood (Figure 3B). This Raman spectroscopy analysis provides valuable insights into the specific alterations in lignin distribution within the wood structure resulting from genome editing. To further investigate this phenomenon, Raman imaging was employed to assess the distribution of lignin in the wild-type wood and 4CL1 knockout wood. The Raman images were generated based on the 1,600 cm⁻¹ peak in the Raman spectra. In these images, the dark blue color corresponds to the wood cells, while the sky blue color represents the lignin. The brightness of the sky blue color indicates the lignin content, with brighter shades indicating higher lignin levels. Figures 3C and 3D exhibit distinct variations in the lignin content between the cell walls and cell corners of the two wood types. Specifically, we observed that the lignin content in 4CL1 knockout wood is lower than in wild-type wood at the cell corners. However, in the cell walls, there seems to be little difference in lignin content between the two types of wood. These Raman imaging data highlight the successful reduction of lignin in the 4CL1 knockout wood, particularly at the cell corners, showcasing the potential impact of genetic engineering on modifying lignin distribution within the wood structure.

Furthermore, we utilized 2D heteronuclear single quantum coherence (HSQC) nuclear magnetic resonance (NMR) spectroscopy to investigate potential differences in lignin structure between wild-type wood and 4CL1 knockout wood. The NMR data revealed slight changes in lignin compositions. Specifically, the percentage of the phenylcoumaran (β -5) structure remained unchanged, but resolin (β - β) decreased in the 4CL1 knockout wood. Conversely, β -O-4 structures exhibited a slight increase (Figure 3E). Interestingly, pBA also increased in the 4CL knockout wood, which aligns with similar results observed in C₃H downregulation (Figure 3F).³⁶ These results demonstrate that the genome editing of 4CL1 not only decreases the lignin content of wood but also modifies the lignin structures. This modification should facilitate the fabrication of densified wood without the need for chemical treatment. The ability to alter both lignin content and structure through genome editing opens up promising avenues for developing sustainable and environmentally friendly methods to produce high-performance densified wood materials.

After characterizing the 4CL1 knockout wood, we utilized it to prepare densified wood. However, unlike previous methods, we did not apply a chemical delignification treatment, as the 12.8% decrease in the lignin content in the 4CL1 knockout wood should be sufficient to enable densification of the wood structure.³ First, we softened the wood samples by soaking the 4CL1 knockout wood and wild-type wood in water under vacuum for 24 h (Figure 4A). The 4CL1 knockout wood becomes noticeably softer than the wild-type wood. When we try to bend the wood samples by hand, the 4CL1 knockout wood can be bent to a great extent, without any visible cracks, while the wild-type wood breaks when bent to the same extent (Figures 4B and S11). We attribute this difference to the lignin reduction in the 4CL1 knockout wood. Additionally, a three-point bending test shows the 4CL1 knockout wood has a much lower flexural strength (17.3 ± 2.1 MPa) than that of the wild-type wood (35.8 ± 1.4 MPa) after soaking with water (Figure 4C). After soaking, the samples were pressed under a pressure of 5 MPa at 120°C for 1 h to form the densified wood. Intriguingly, SEM reveals the densified 4CL1 knockout wood (Figure 4E)

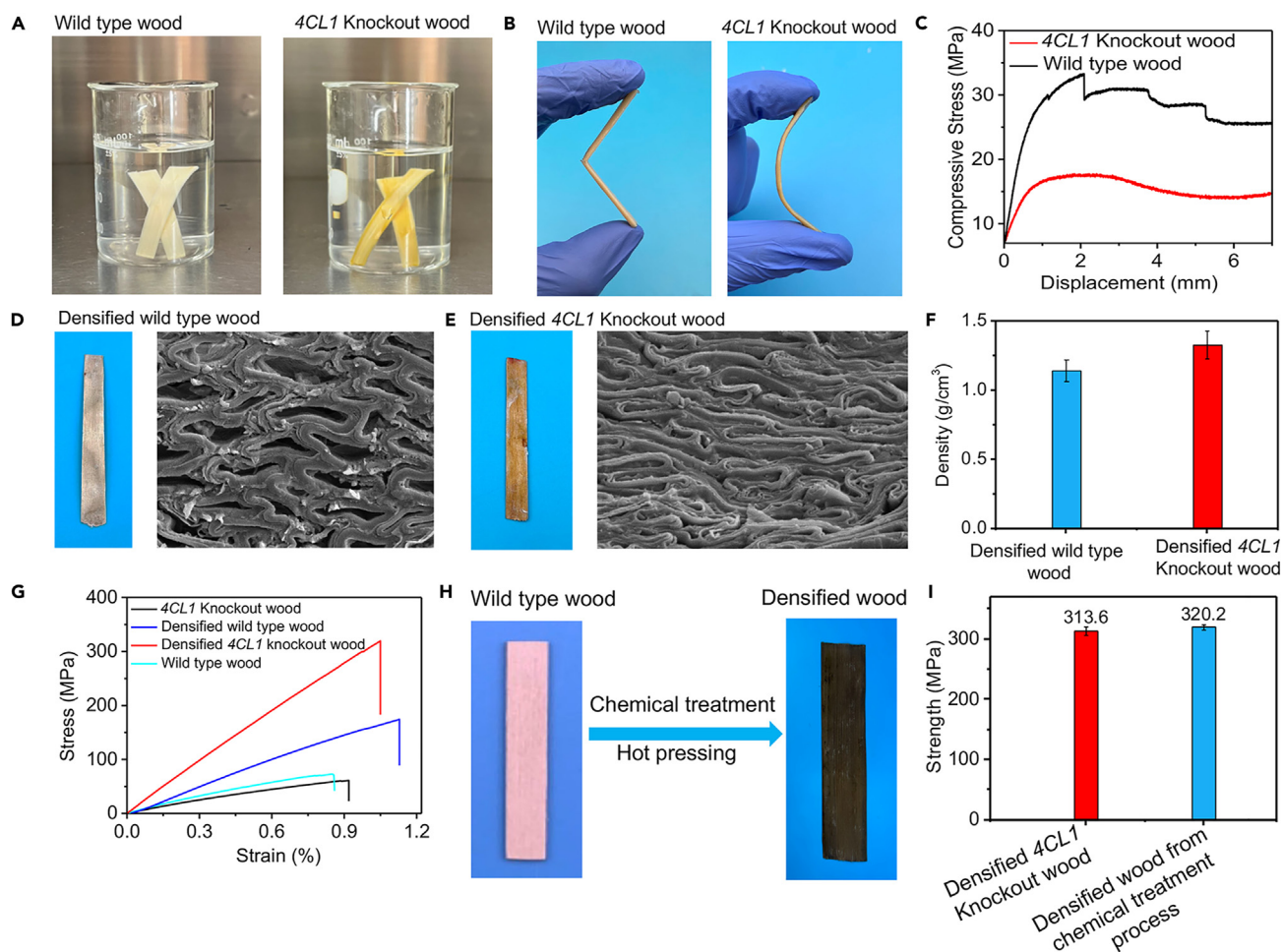


Figure 4. Fabrication and performance of densified wood produced using wild-type wood and 4CL1 knockout wood as starting materials

- (A) Photographs of the wild-type wood and 4CL1 knockout wood soaking in water under vacuum.
- (B) Photographs showing the 4CL1 knockout wood is much softer after soaking in water for 24 h.
- (C) Flexural strength of the wild-type wood and 4CL1 knockout wood after soaking in water.
- (D and E) Photograph and SEM image of the (D) densified wild-type wood and (E) densified 4CL1 knockout wood.
- (F) Comparison of the density of the densified wild-type wood and densified 4CL1 knockout wood.
- (G) The stress-strain curves of wild-type wood, 4CL1 knockout wood, densified wild-type wood, and densified 4CL1 knockout wood.
- (H) Photos show the fabrication of densified wood from wild-type wood through a conventional process by chemical treatment and hot pressing.
- (I) Comparison of the tensile strength of the densified wood from wild-type wood though a conventional process and densified 4CL1 knockout wood from waste-free process.

Data are represented as mean \pm SEM.

possesses a significantly denser microstructure than that of the densified wild-type wood (Figure 4D). The densified 4CL1 knockout wood exhibits a higher density ($1.32 \text{ g}/\text{cm}^3$) than that of the densified wild-type wood ($1.15 \text{ g}/\text{cm}^3$) (Figure 4F). As a result, although the 4CL1 knockout wood displays a decreased tensile strength, after being densified, the tensile strength of the densified 4CL1 knockout wood shows a marked increase of 5.6 times higher than that of the natural 4CL1 knockout wood (Figures 4G and S12). In contrast, the densified wild-type wood shows an increase of just 2.6 times higher than that of wild-type wood, due to the high lignin content, which decreases how much the material can be densified (Figure S12).

In addition, the tensile strength of the densified 4CL1 knockout wood is about 1.6 times higher than that of the densified wild-type wood (Figures 4G and S12).

Figures 4G and S12 illustrate the results obtained regarding the tensile strength of the different wood samples. The data reveal interesting findings. Firstly, the tensile strength of genetically engineered (4CL1 knockout) wood is initially lower than that of natural 4CL1 knockout wood. However, after undergoing the densification process, the tensile strength of densified 4CL1 knockout wood significantly increases, reaching a value approximately 5.6 times higher than that of the natural 4CL1 knockout wood. In contrast, the densified wild-type wood exhibits a more moderate improvement in tensile strength, measuring approximately 2.6 times higher than the original wild-type wood. This difference can be attributed to the higher lignin content in wild-type wood, which limits the extent to which the material can be effectively densified. Additionally, when comparing the tensile strength of densified 4CL1 knockout wood with densified wild-type wood, the former demonstrates approximately 1.6 times higher tensile strength. In addition, the densified 4CL1 knockout wood demonstrates a flexural strength of 278.3 ± 9.7 MPa (**Figure S13**). These results highlight the positive impact of genetic engineering and the densification process on enhancing the tensile strength of wood materials. Furthermore, a densified wood was fabricated from wild-type wood through the conventional method that includes chemical treatment, resulting in the removal of 12.4% of lignin, mimicking the lignin reduction impact of the genome-editing process, followed by hot pressing (**Figure 4H**). The resulting densified wood exhibits a tensile strength of 320.2 ± 3.5 MPa, closely resembling the tensile strength of densified 4CL1 knockout wood (**Figure 4I**). This implies that the genome-editing process achieves a similar effect to chemical treatment in reducing wood lignin content but with the additional advantage of being more environmentally friendly. Lignin, being a rigid polymer, can hinder cell wall deformation and restrict the rearrangement of cellulose fibers. With lower lignin content, the cell walls become more flexible and capable of undergoing greater deformation, leading to increased densification and improved strength. In addition, a lower lignin content allows for better contact and bonding between cellulose fibers in densified wood. When the lignin content is reduced, the fibers have more opportunities to come into direct contact and establish stronger bonding interfaces. This improved fiber bonding enhances load transfer within the material, resulting in higher strength and improved mechanical properties. During the densified wood fabrication process, no chemicals were used, and no environmentally harmful waste is produced, making this a green method of wood engineering. These findings indicate that genome editing is a promising method for creating optimal wood feedstock, particularly for chemical-free wood engineering.

Conclusion

We demonstrated a waste-free process for wood engineering by reducing the lignin content of poplar wood through a genome-editing technology. The results show that the 4CL1 knockout wood does not show a significant change in plant growth except for a 12.8% reduction in lignin content. The densified 4CL1 knockout wood is fabricated by a waste-free process through soaking the 4CL1 knockout wood in water followed by hot pressing. The resulting material exhibits a tensile strength of 313.6 ± 6.4 MPa, which is 5.6 and 1.6 times higher than that of the natural 4CL1 knockout wood and densified wild-type wood. In addition, the tensile strength of the densified 4CL1 knockout wood is comparable to that of the densified wood (320.2 ± 3.5 MPa) from wild-type wood using a conventional manufacturing process involving chemical treatment followed by densification. This indicates that the genome-editing process achieves a similar impact to the chemical treatment in reducing lignin content in wood. This work demonstrates that using genome editing to engineer poplar wood with less lignin content can eliminate the chemical delignification step in traditional wood engineering processes, providing a cost-effective

and environmentally friendly method to produce products like densified wood. In addition, the successful application of genome editing to engineer wood with reduced lignin content opens up possibilities for the development of other engineered wood materials with enhanced properties, such as improved durability, and modified thermal or acoustic characteristics. In summary, the utilization of 4CL1 knockout poplar or other trees as feedstocks for the production of high-performance, sustainable, and value-added wood-based materials holds great promise, as demonstrated in this study as well as in a recent study that reported more efficient fiber pulping via multiplexed genome editing.²² This approach of coupling elite wood materials generated by genetic engineering with wood engineering has the potential to contribute to the development of a future CO₂-negative bioeconomy by providing renewable and environmentally friendly alternatives to traditional materials.

EXPERIMENTAL PROCEDURES

Resource availability

Lead contact

Requests for more information and resources should be directed to and will be fulfilled by the lead contact, Liangbing Hu (binghu@umd.edu).

Materials availability

All genome-editing plasmids are available at Addgene (https://www.addgene.org/Yiping_Qi/).

Data and code availability

This article did not generate any code. All data reported in this article will be shared by the lead contact upon request.

Plasmid construction

The genomic sequence for *Populus tremula* × *P. alba* 4CL1 gene (PtXaTreH.01G031400 and PtXaAlbH.01G031600) was obtained from Phytozome (<https://phytozome-next.jgi.doe.gov/>). The multiplexed C-to-T base editing T-DNA vector was constructed using the CRISPR tools we previously reported.^{24,37} To introduce pre-mature stop codons, two gRNAs, each with a 20 bp protospacer, were designed to target both alleles of the 4CL1 gene at the first exon (Table S1). Each gRNA was synthesized as two reverse complementary oligonucleotides and then annealed. Annealed gRNA oligonucleotides were ligated into gRNA entry plasmids pYPQ131A (Addgene #69273) and pYPQ132B (Addgene #69282), respectively. Then, these two gRNA clones were assembled by Golden Gate Cloning into pYPQ142 (Addgene #69294) to generate the gRNA entry clone. This gRNA entry clone, hA3A-Y130F-based SpCas9n CBE entry clone (pYPQ265E2, Addgene #164719), and pYPQ202 (Addgene #86198) were used to prepare the T-DNA expression vector by the three-way Gateway LR reaction. The resulting T-DNA vector was transformed into *Agrobacterium* strain GV3101 followed by poplar transformation.

Poplar transformation and genotyping

Populus tremula × *P. alba* hybrid clone INRA 717-1B4 was used for *Agrobacterium*-mediated transformation, as described previously.³⁸ Transformed plants were selected on shoot induction medium and root medium containing 20 mg/L hygromycin and 200 mg/L Timentin. Leaf tissue of transgenic plants was collected for DNA extraction. To analyze the genotype of transgenic CBE plants, PCR was conducted using Phire tissue direct PCR master mix (Thermo Scientific, USA) using specific primers (Table S2). PCR products were enzymatically purified using Exonuclease I

and Quick CIP (NEB, USA). Purified PCR products were used for Sanger sequencing (Genewiz, USA) to reveal the genotypes.

Fabrication process of the densified wood

The wild-type wood and 4CL1 knockout wood strips were soaked in water for 24 h under vacuum, followed by hot pressing at 120°C under a pressure of about 5 MPa for 1 h to form the densified wild-type wood and 4CL1 knockout wood.

The wild-type wood was immersed in a boiling solution containing a mixture of 2.5 M NaOH and 0.4 M Na₂SO₃ for 1 h, after which it underwent multiple immersions in boiling deionized (DI) water to eliminate residual chemicals. Subsequently, the wood blocks were subjected to pressing at 120°C under 5 MPa pressure for 1 h to produce the densified wood.

Characterization of the wood microstructures

The microstructures of the wood samples and super wood tubes were observed by a Hitachi SU-70 SEM.

Measurement of the lignin content

The lignin contents were measured based on Technical Association of Pulp and Paper Industry Standard Method T 222-om-83. 1 g dry wood (m_0) was extracted with ethanol alcohol for 4 h to remove extracts such as resin, fat, and wax. The wood powder after extraction was treated with cold H₂SO₄ (72%, 15 mL) for 2 h with vigorous stirring at 20°C. The mixtures were transferred to a beaker and diluted to 3 wt % H₂SO₄ by adding 560 mL of DI water and boiled for 4 h. Finally, the solution was filtered and washed with DI water. The insoluble materials were dried and weighed (m_1). The lignin content was calculated as $[m_1/m_0] \times 100\%$.

Mechanical measurements of the densified wood

The tensile and compressive properties of the samples were measured using an Instron 5565 universal tester with a 30 kN load cell. The dimensions of the tensile samples were approximately 100 × 5 × 0.15 mm. The samples were clamped at both ends and stretched along the wood fiber direction with a constant test speed of 2 mm min⁻¹ at room temperature.

WAXD

WAXD experiments were carried out using an in-house instrument (XEUSS 2.0, Xonics) at an X-ray wavelength of 1.54 Å. The X-ray beam diameter was 0.8 mm, and the sample-to-detector distance (SDD) was 133 mm. A Dectris Pilatus 300k detector (Dectris, Switzerland) was employed to register 2D diffraction patterns. The SDD and X-ray beam center were calibrated using silver behenate powder. The conversion of 2D scattering pattern to 1D traces was performed using NIKA and Fit2D packages.

2D HSQC NMR

The NMR experiments using 2D HSQC were conducted on enzyme lignins (ELs) following previous methods.^{39–41} NMR tubes containing 50 mg ball-milled whole-cell walls and 35 mg ELs were prepared with DMSO-d₆:pyridine-d₅ (4:1, v/v) for gel-NMR experiments. The central DMSO solvent peak (δ_C 39.5, δ_H 2.49 ppm) was used as the internal reference. The NMR data were collected using a Bruker Biospin (Billerica, MA, USA) Avance NEO 700 MHz spectrometer equipped with a 5 mm QCI ¹H/³¹P/¹³C/¹⁵N cryoprobe with inverse geometry. An adiabatic ¹H-¹³C 2D HSQC experiment (hsqcetgpsisp2.2) from Bruker was performed as described in previous

publications.^{39,41} For the EL samples, the 2D HSQC experiments were acquired in the range of 11.5 to −0.5 ppm (12 ppm spectral width) in F2 (¹H) with 3,448 data points (acquisition time, 200 ms) and 215 to −5 ppm (220 ppm spectral width) in F1 (¹³C) with 618 increments (F1 acquisition time, 8.0 ms) of 32 scans with a 1 s inter-scan delay (D1); the d24 delay was 0.89 ms (1/8 J, J = 145 Hz). The total acquisition time for each sample was 7 h. The volume integration of contours in the 2D HSQC plots was conducted using TopSpin 4.1.4 software (Mac version) from Bruker, without the use of correction factors. To quantify the aromatic H/G/S signals, the H_{2/6} and S_{2/6} correlations were used, and the G₂ integrals were doubled to be on the same atom basis (S_{2/6} + S'_{2/6} + H_{2/6} + 2G₂ = 100%). For the estimation of the various aliphatic interunit linkage types, the well-resolved α -C/H peaks were measured, and the relative percentages were reported based on a 2A _{α} + 2B _{α} + C _{α} = 100% basis (A, β -ether; B, phenylcoumaran; C, resolin).

Raman

A Yvon Jobin LabRam ARAMIS confocal Raman microscope (Horiba, France) was used to map the cross-sections of wild-type wood and 4CL1 knockout wood to assess the distribution of lignin across the cell walls before and after delignification. The samples used for the Raman mapping measurements were 20 μ m thick, sandwiched between a glass slide and a coverslip, in a wet state. The laser wavelength was 532 nm. Mapping was performed at a step size of 300 nm, with an exposure time of 0.2 s (50% attenuation), under StreamlineHR mode. The size of a typical measurement area was 30 × 30 μ m. Data collection and post-processing were performed using the Labspec 5.0 software (Horiba, France).

SUPPLEMENTAL INFORMATION

Supplemental information can be found online at <https://doi.org/10.1016/j.matt.2024.07.003>.

ACKNOWLEDGMENTS

This work is not directly funded. L.H. acknowledges support from the University of Maryland A. James Clark School of Engineering. NMR data were acquired on the Bruker Avance NEO 700 MHz instrument at the NMR facility of the Wisconsin Energy Institute (WEI) of the University of Wisconsin–Madison. H.K. was funded by the DOE BER Office of Science (DE-SC0018409) and supported in part by the US Department of Agriculture, US Forest Service. Y.Q. acknowledges the support of the NSF Plant Genome Research Program grant (IOS-2132693) and the DOE BER Office of Science (DE-SC0023011). The Xenocs Xeuss small-angle X-ray instrument was purchased under NSF award no. 1228957. The identification of any commercial product or trade name does not imply endorsement or recommendation by the National Institute of Standards and Technology.

AUTHOR CONTRIBUTIONS

L.H., Y.Q., and Y.L. conceived the idea and designed the experiments. Y.L. and G.L. contributed to the 4CL1 knockout wood production, fabrication, and characterization. Y.G. contributed to testing the lignin content of the wood samples. Y.G., D.W., and S.v.K. contributed to collection of the SEM and digital images. Y.M. and M.Z. contributed to the LAMAN measurement and analysis. Y.M. contributed to wide-angle X-ray scattering measurements. X.P. and H.K. contributed to 2D HSQC NMR measurements. T.M. provided characterization via FTIR. Y.L., A.B., G.L., Y.Q., and L.H. collaboratively analyzed the data and wrote the manuscript. All authors commented on the final manuscript.

DECLARATION OF INTERESTS

We, the authors, have a patent application: US provisional application no. 63/384578. Title: Genetically Edited Trees for Strong Wood and Other Engineered Wood. Filing date: November 21, 2022. Inventors: L.H., Y.L., Y.M., Y.Q., and G.L.

Received: March 31, 2024

Revised: June 11, 2024

Accepted: July 4, 2024

Published: August 12, 2024

REFERENCES

- Ding, Y., Pang, Z., Lan, K., Yao, Y., Panzarasa, G., Xu, L., Lo Ricco, M., Rammer, D.R., Zhu, J.Y., Hu, M., et al. (2023). Emerging Engineered Wood for Building Applications. *Chem. Rev.* 123, 1843–1888. <https://doi.org/10.1021/acs.chemrev.2c00450>.
- Chen, C., Kuang, Y., Zhu, S., Burgert, I., Keplinger, T., Gong, A., Li, T., Berglund, L., Eichhorn, S.J., and Hu, L. (2020). Structure–property–function relationships of natural and engineered wood. *Nat. Rev. Mater.* 5, 642–666. <https://doi.org/10.1038/s41578-020-0195-z>.
- Song, J., Chen, C., Zhu, S., Zhu, M., Dai, J., Ray, U., Li, Y., Kuang, Y., Li, Y., Quispe, N., et al. (2018). Processing bulk natural wood into a high-performance structural material. *Nature* 554, 224–228. <https://doi.org/10.1038/nature25476>.
- Fang, Z., Li, B., Liu, Y., Zhu, J., Li, G., Hou, G., Zhou, J., and Qiu, X. (2020). Critical Role of Degree of Polymerization of Cellulose in Super-Strong Nanocellulose Films. *Matter* 2, 1000–1014. <https://doi.org/10.1016/j.matt.2020.01.016>.
- Li, T., Zhai, Y., He, S., Gan, W., Wei, Z., Heidarinejad, M., Dalgo, D., Mi, R., Zhao, X., Song, J., et al. (2019). A radiative cooling structural material. *Science* 364, 760–763. <https://doi.org/10.1126/science.aau9101>.
- Sun, H., Ji, T., Zhou, X., Bi, H., Xu, M., Huang, Z., and Cai, L. (2021). Mechanically strong, transparent, and biodegradable wood-derived film. *Mater. Chem. Front.* 5, 7903–7909. <https://doi.org/10.1039/d1qm00973g>.
- Li, K., Wang, S., Chen, H., Yang, X., Berglund, L.A., and Zhou, Q. (2020). Self-Densification of Highly Mesoporous Wood Structure into a Strong and Transparent Film. *Adv. Mater.* 32, 2003653. <https://doi.org/10.1002/adma.202003653>.
- Li, Y., Fu, Q., Yu, S., Yan, M., and Berglund, L. (2016). Optically Transparent Wood from a Nanoporous Cellulosic Template: Combining Functional and Structural Performance. *Biomacromolecules* 17, 1358–1364. <https://doi.org/10.1021/acs.biomac.6b00145>.
- Fundamentals of Thermochemical Biomass Conversion (1985). , R.P. Overend, T.A. Milne, and L.K. Mudge, eds. (Springer Netherlands). <https://doi.org/10.1007/978-94-009-4932-4>.
- Zhu, M., Song, J., Li, T., Gong, A., Wang, Y., Dai, J., Yao, Y., Luo, W., Henderson, D., and Hu, L. (2016). Highly Anisotropic, Highly Transparent Wood Composites. *Adv. Mater.* 28, 5181–5187. <https://doi.org/10.1002/adma.201600427>.
- Liu, Y., Li, B., Mao, W., Hu, W., Chen, G., Liu, Y., and Fang, Z. (2019). Strong Cellulose-Based Materials by Coupling Sodium Hydroxide-Anthraquinone (NaOH-AQ) Pulp with Hot Pressing from Wood. *ACS Omega* 4, 7861–7865. <https://doi.org/10.1021/acsomega.9b00411>.
- Zhu, M., Wang, Y., Zhu, S., Xu, L., Jia, C., Dai, J., Song, J., Yao, Y., Wang, Y., Li, Y., et al. (2017). Anisotropic, Transparent Films with Aligned Cellulose Nanofibers. *Adv. Mater.* 29, 10. <https://doi.org/10.1002/adma.201606284>.
- Muurinen, E. (2000). Organosolv pulping: a review and distillation study related to peroxyacid pulping (Oulun yliopisto). <https://urn.fi/URN:ISBN:9514256611>.
- Pan, X., Arato, C., Gilkes, N., Gregg, D., Mabee, W., Pye, K., Xiao, Z., Zhang, X., and Saddler, J. (2005). Biorefining of softwoods using ethanol organosolv pulping: Preliminary evaluation of process streams for manufacture of fuel-grade ethanol and co-products. *Biotechnol. Bioeng.* 90, 473–481. <https://doi.org/10.1002/bit.20453>.
- Fort, D.A., Remsing, R.C., Swatloski, R.P., Moyna, P., Moyna, G., and Rogers, R.D. (2007). Can ionic liquids dissolve wood? Processing and analysis of lignocellulosic materials with 1-n-butyl-3-methylimidazolium chloride. *Green Chem.* 9, 63–69. <https://doi.org/10.1039/b607614a>.
- Liu, J., Takada, R., Karita, S., Watanabe, T., Honda, Y., and Watanabe, T. (2010). Microwave-assisted pretreatment of recalcitrant softwood in aqueous glycerol. *Bioresour. Technol.* 101, 9355–9360. <https://doi.org/10.1016/j.biortech.2010.07.023>.
- Lin, X., Wu, Z., Zhang, C., Liu, S., and Nie, S. (2018). Enzymatic pulping of lignocellulosic biomass. *Ind. Crops Prod.* 120, 16–24. <https://doi.org/10.1016/j.indcrop.2018.04.033>.
- Ab Rasid, N.S., Shamjuddin, A., Abdul Rahman, A.Z., and Amin, N.A.S. (2021). Recent advances in green pre-treatment methods of lignocellulosic biomass for enhanced biofuel production. *J. Clean. Prod.* 321, 129038. <https://doi.org/10.1016/j.jclepro.2021.129038>.
- Tsai, C.J., Xu, P., Xue, L.J., Hu, H., Nyamdar, B., Naran, R., Zhou, X., Goeminne, G., Gao, R., Gjersing, E., et al. (2020). Compensatory guaiacyl lignin biosynthesis at the expense of syringyl lignin in 4CL1-knockout poplar. *Plant Physiol.* 183, 123–136. <https://doi.org/10.1104/pp.19.01550>.
- Sun, H., Li, Y., Feng, S., Zou, W., Guo, K., Fan, C., Si, S., and Peng, L. (2013). Analysis of five rice 4-coumarate: Coenzyme A ligase enzyme activity and stress response for potential roles in lignin and flavonoid biosynthesis in rice. *Biochem. Biophys. Res. Commun.* 430, 1151–1156. <https://doi.org/10.1016/j.bbrc.2012.12.019>.
- Sun, H., Guo, K., Feng, S., Zou, W., Li, Y., Fan, C., and Peng, L. (2015). Positive selection drives adaptive diversification of the 4-coumarate: CoA ligase (4CL) gene in angiosperms. *Ecol. Evol.* 5, 3413–3420. <https://doi.org/10.1002/ece3.1613>.
- Sulis, D.B., Jiang, X., Yang, C., Marques, B.M., Matthews, M.L., Miller, Z., Lan, K., Cofre-Vega, C., Liu, B., Sun, R., et al. (2023). Multiplex CRISPR editing of wood for sustainable fiber production. *Science* 381, 216–221. <https://doi.org/10.1126/science.add4514>.
- Li, X., Weng, J.K., and Chapple, C. (2008). Improvement of biomass through lignin modification. *Plant J.* 54, 569–581. <https://doi.org/10.1111/j.1365-313X.2008.03457.x>.
- Li, G., Sretenovic, S., Eisenstein, E., Coleman, G., and Qi, Y. (2021). Highly efficient C-to-T and A-to-G base editing in a *Populus* hybrid. *Plant Biotechnol. J.* 19, 1086–1088. <https://doi.org/10.1111/pbi.13581>.
- Ren, Q., Sretenovic, S., Liu, G., Zhong, Z., Wang, J., Huang, L., Tang, X., Guo, Y., Liu, L., Wu, Y., et al. (2021). Improved plant cytosine base editors with high editing activity, purity, and specificity. *Plant Biotechnol. J.* 19, 2052–2068. <https://doi.org/10.1111/pbi.13635>.
- Lee, S.H., Saito, Y., Sakai, T., and Utsunomiya, H. (2002). Microstructures and mechanical properties of 6061 aluminum alloy processed by accumulative roll-bonding. *Mater. Sci. Eng. A* 325, 228–235. [https://doi.org/10.1016/S0921-5093\(01\)01416-2](https://doi.org/10.1016/S0921-5093(01)01416-2).
- Vanholme, R., Demedts, B., Morreel, K., Ralph, J., and Boerjan, W. (2010). Lignin biosynthesis and structure. *Plant Physiol.* 153, 895–905. <https://doi.org/10.1104/pp.110.155119>.
- Vanholme, R., De Meester, B., Ralph, J., and Boerjan, W. (2019). Lignin biosynthesis and its integration into metabolism. *Curr. Opin.*

- Biotechnol. 56, 230–239. <https://doi.org/10.1016/j.copbio.2019.02.018>.
29. Zhou, X., Jacobs, T.B., Xue, L.-J., Harding, S.A., and Tsai, C.-J. (2015). Exploiting SNPs for biallelic CRISPR mutations in the outcrossing woody perennial *Populus* reveals 4-coumarate: CoA ligase specificity and redundancy. New Phytol. 208, 298–301. <https://doi.org/10.2307/newphytologist.208.2.298>.
30. Voelker, S.L., Lachenbruch, B., Meinzer, F.C., Jourdes, M., Ki, C., Patten, A.M., Davin, L.B., Lewis, N.G., Tuskan, G.A., Gunter, L., et al. (2010). Antisense down-regulation of 4CL expression alters lignification, tree growth, and saccharification potential of field-grown poplar. Plant Physiol. 154, 874–886. <https://doi.org/10.1104/pp.110.159269>.
31. Mao, Y., Liu, K., Zhan, C., Geng, L., Chu, B., and Hsiao, B.S. (2017). Characterization of Nanocellulose Using Small-Angle Neutron, X-ray, and Dynamic Light Scattering Techniques. J. Phys. Chem. B 121, 1340–1351. <https://doi.org/10.1021/acs.jpcb.6b11425>.
32. Göschel, U., Deutscher, K., and Abetz, V. (1996). Wide-angle X-ray scattering studies using an area detector: crystallite orientation in semicrystalline PET structures. Polymer 37, 1–6. [https://doi.org/10.1016/0032-3861\(96\)81592-8](https://doi.org/10.1016/0032-3861(96)81592-8).
33. Agarwal, U.P. (2006). Raman imaging to investigate ultrastructure and composition of plant cell walls: Distribution of lignin and cellulose in black spruce wood (*Picea mariana*). Planta 224, 1141–1153. <https://doi.org/10.1007/s00425-006-0295-z>.
34. Hänninen, T., Kontturi, E., and Vuorinen, T. (2011). Distribution of lignin and its coniferyl alcohol and coniferyl aldehyde groups in *Picea abies* and *Pinus sylvestris* as observed by Raman imaging. Phytochemistry 72, 1889–1895. <https://doi.org/10.1016/j.phytochem.2011.05.005>.
35. Ozgenc, O., Durmaz, S., Serdar, B., Boyaci, I.H., Eksi-Kocak, H., and Öztürk, M. (2018). Characterization of fossil Sequoiadendron wood using analytical instrumental techniques. Vib. Spectrosc. 96, 10–18. <https://doi.org/10.1016/j.vibspec.2018.02.006>.
36. Kim, H., Li, Q., Karlen, S.D., Smith, R.A., Shi, R., Liu, J., Yang, C., Tunlaya-Anukit, S., Wang, J.P., Chang, H.M., et al. (2020). Monolignol Benzoates Incorporate into the Lignin of Transgenic *Populus trichocarpa* Depleted in C3H and C4H. ACS Sustain. Chem. Eng. 8, 3644–3654. <https://doi.org/10.1021/acssuschemeng.9b06389>.
37. Lowder, L.G., Zhang, D., Baltes, N.J., Paul, J.W., Tang, X., Zheng, X., Voytas, D.F., Hsieh, T.F., Zhang, Y., and Qi, Y. (2015). A CRISPR/Cas9 toolbox for multiplexed plant genome editing and transcriptional regulation. Plant Physiol. 169, 971–985. <https://doi.org/10.1104/pp.15.00636>.
38. Leppla, J.C., Cristina, A., Brasileiro, M., Michel, M.F., Delmotte, F., and Jouanin, L. (1992). Transgenic poplars: expression of chimeric genes using four different constructs. Plant Cell Rep. 11, 137–141. <https://doi.org/10.1007/BF00232166>.
39. Kim, H., Padmakshan, D., Li, Y., Rencoret, J., Hatfield, R.D., and Ralph, J. (2017). Characterization and Elimination of Undesirable Protein Residues in Plant Cell Wall Materials for Enhancing Lignin Analysis by Solution-State Nuclear Magnetic Resonance Spectroscopy. Biomacromolecules 18, 4184–4195. <https://doi.org/10.1021/acs.biomac.7b01223>.
40. Kim, H., Ralph, J., and Akiyama, T. (2008). Solution-state 2D NMR of Ball-milled Plant Cell Wall Gels in DMSO-d₆. Bioenergy Res. 1, 56–66. <https://doi.org/10.1007/s12155-008-9004-z>.
41. Kim, H., and Ralph, J. (2010). Solution-state 2D NMR of ball-milled plant cell wall gels in DMSO-d₆/pyridine-d₅. Org. Biomol. Chem. 8, 576–591. <https://doi.org/10.1039/b916070a>.